Impact of RCS Temperature Program on the Neutronic Characteristics of a Soluble-Boron-Free SMR Core

Yu Yeon Cho [a], Seongho Park [a], Junggyu Lee [a]
[a]*KEPCO Nuclear Fuel, 242, Daedeok-daero 989 beon-gil, Yuseong-gu, Daejeon 34057, Republic of Korea*
[*]*Corresponding author: yycho@knfc.co.kr*

***Keywords :** i-SMR, RCS temperature program, Reactivity control

1. Introduction

In the previous study [1], the i-SMR adopted an RCS temperature program where the average coolant temperature decreases linearly as power increases. This strategy was designed to facilitate reactivity control by leveraging the strongly negative Moderator Temperature Coefficient (MTC) inherent in soluble boron-free cores [2]. In contrast, most commercial nuclear power plants maintain a constant coolant inlet temperature, resulting in a temperature profile where the average coolant temperature rises with power.

This work aims to evaluate the impact of applying a l commercial reactor's RCS temperature program (Constant T_{in}) on the neutronic characteristics of an Soluble-Boron-Free SMR core, comparing it with the previously established program (Sliding T_{in}). The analysis is conducted for both the initial core cycle (1st cycle) and the equilibrium core cycle (8th cycle).

2. Methods

2.1 Computational Methods

Assembly burnup calculations for two group cross section generation were calculated by KARMA (Kernel Analyzer by Ray-tracing Method for fuel Assembly) [3, 4] which is a two-dimensional multi-group lattice transport code. KARMA includes the ENDF/B-VII.1 based 190 group and 47 group cross section library. This code uses the subgroup method for resonance self-shielding effect and MOC (Method of Characteristics) as the transport solution method.

ASTRA (Advanced Static and Transient Reactor Analyzer) code was used for three-dimensional core calculation [5]. This code is a 3D core depletion code and developed by KEPCO NF (KEPCO Nuclear Fuel) as a nuclear design code for the core design of pressurized water reactors (PWRs) based on the reactor physics technologies. It adopts a Semi-Analytic Nodal Method (SANM) formulated with the Coarse-Mesh Finite Difference method (CMFD) as the neutronics solver for the reactor core analysis [6, 7].

2.2 Core Design and RCS Temperature Program

The i-SMR is designed for a thermal power output of 520 MW. The core consists of 69 assemblies arranged in a 17 × 17 lattice. The active core height is 240 cm divided into 24 axial meshes. The burnable absorber utilized enriched gadolinium oxide (Gd2O3) at a concentration of 8 wt.% or less.

The control rods for regulation, which consist of 28 Ag-In-Cd (AIC) pins, are classified into four groups—R4, R3, R2, and R1—, based on their insertion order. During power operation, the three groups—R4, R3, and R2—are typically inserted and withdrawn with an overlap length of 120 cm. Fig. 1 depicts the radial configuration of the regulation bank of i-SMR core.

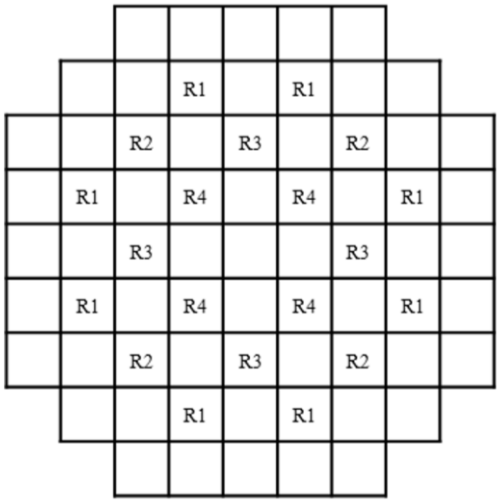

Fig. 1. Radial configuration of Regulation Bank of i-SMR core

As discussed in the introduction, this study compares two distinct coolant temperature program concepts: 1) Sliding T_{in} and 2) Constant T_{in}. For the Constant T_{in} case (Case 2), the inlet temperature was fixed at 286.0 ℃, which corresponds to the full-power inlet temperature of the Sliding T_{in} concept (Case 1). The core depletion calculations were performed based on these profiles, and the power-dependent coolant inlet temperatures for both cases are shown in Fig. 2.

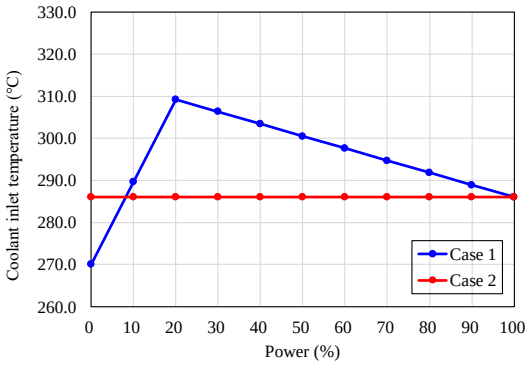

Fig. 2. Power dependent coolant inlet temperature

3. Results and Analysis

3.1 Excess Reactivity Variation on Daily Load follow Operation

For the daily load-follow simulation, we adopted a 2-4-2-16 hour operational strategy. The core analysis was performed at selected target power levels of 20%, 50%, and 75%.

To illustrate the load-follow scenario at a target power of 50%, the operational sequence was defined as follows: the core power was reduced from 100% to 50% over a 2 hours, maintained at the 50% level for 4 hours, and then ramped back up to 100% over the next 2 hours. Finally, the reactor was held at full power for the remaining 16 hours to complete a 24-hour cycle. Under the condition of control rods being fixed at the initial critical state, this evaluation involved calculating eigenvalues corresponding to power changes over time.

Fig. 3, 4 and 5 show that the net change of reactivity with the power change in the 1st cycle for the Case 1. The variations in excess reactivity following power changes exhibit similar trends across all scenarios. However, the magnitude of these variations increases as the target power level decreases. The highest net excess reactivity of 784.3 pcm occurs at BOC under the 100-20-100% load-follow sequence.

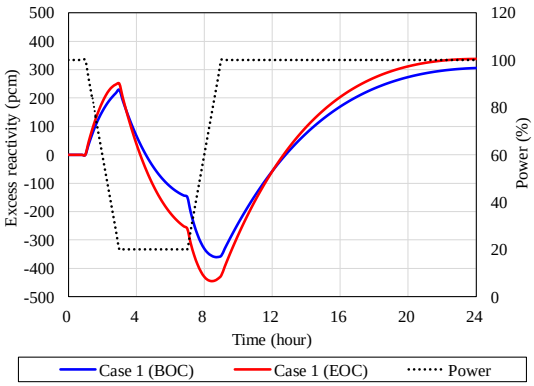

Fig. 3. The reactivity variation with power change (1st cycle, 100-20-100% power changes, Case 1)

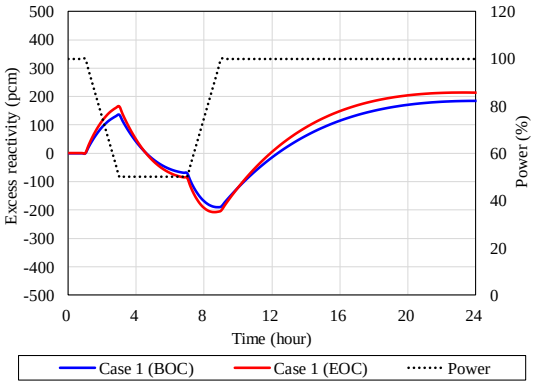

Fig. 4. The reactivity variation with power change (1st cycle, 100-50-100% power changes, Case 1)

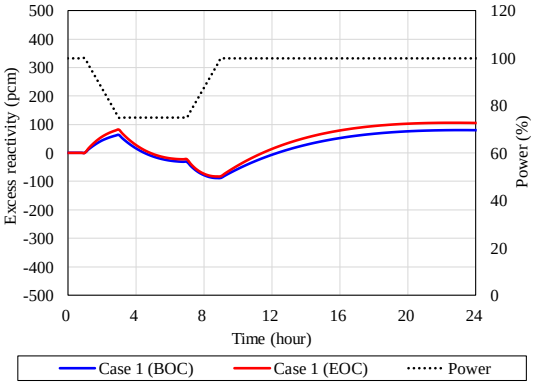

Fig. 5. The reactivity variation with power change (1st cycle, 100-75-100% power changes, Case 1)

Fig. 6, 7 and 8 show that the net change of reactivity with the power change in the 1st cycle for the Case 2. The reactivity swings in the Case 2 are much more pronounced because the average coolant temperature decreases sharply as power drops, triggering a massive positive reactivity feedback due to the strong negative MTC. In contrast, the Case 1 exhibits a relatively stable reactivity profile because its temperature program keeps the average temperature almost constant. The largest maximum net excess reactivity was observed at EOC under the 100-20-100% scenario, reaching 2089.9 pcm.

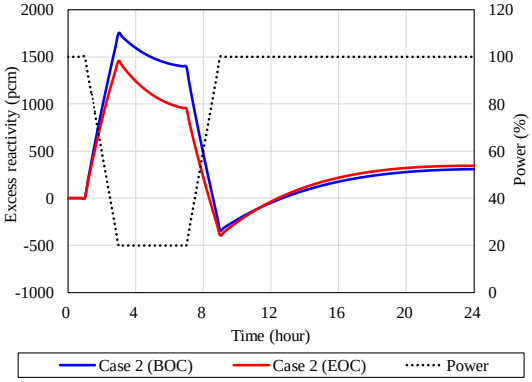

Fig. 6. The reactivity variation with power change (1st cycle, 100-20-100% power changes, Case 2)

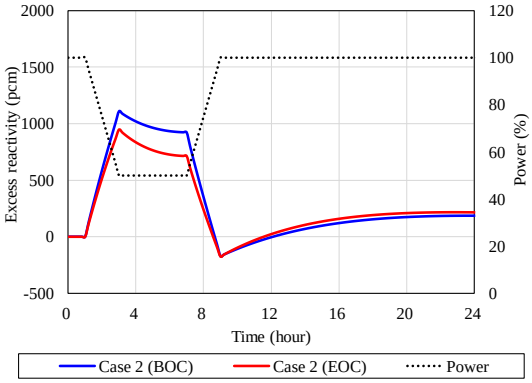

Fig. 7. The reactivity variation with power change (1st cycle, 100-50-100% power changes, Case 2)

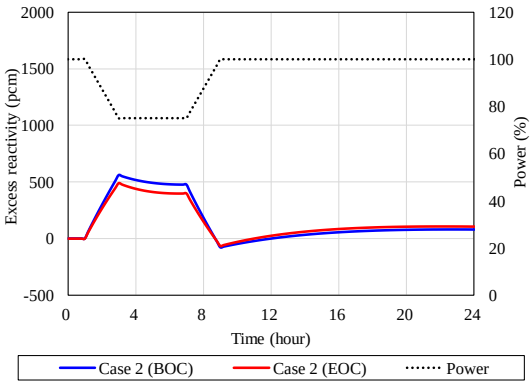

Fig. 8. The reactivity variation with power change (1st cycle, 100-75-100% power changes, Case 2)

Figs. 9, 10 and 11 illustrate the net reactivity changes for the Case 1 during the 8th cycle. Compared to the initial core, the difference in the excess reactivity between BOC and EOC is more pronounced in the equilibrium cycle. Specifically, the maximum net excess reactivity of 766.9 pcm was recorded at EOC under the 100-20-100% load-follow scenario.

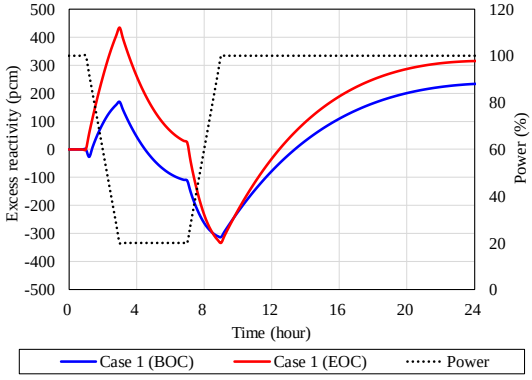

Fig. 9. The reactivity variation with power change (8th cycle, 100-20-100% power changes, Case 1)

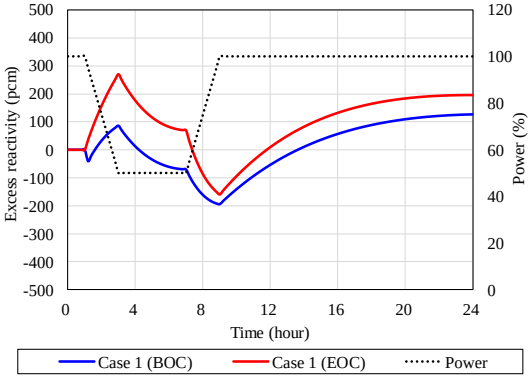

Fig. 10. The reactivity variation with power change (8th cycle, 100-50-100% power changes, Case 1)

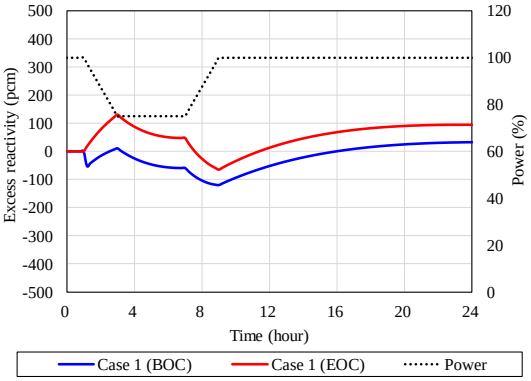

Fig. 11. The reactivity variation with power change (8th cycle, 100-75-100% power changes, Case 1)

Fig. 12, 13 and 14 illustrate that the net reactivity changes versus the power change in the 8th cycle for the Case 2. The largest maximum net excess reactivity was observed at EOC under the 100-20-100% scenario, reaching 2025.3 pcm.

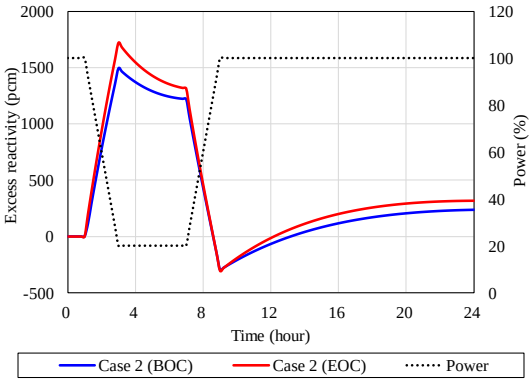

Fig. 12. The reactivity variation with power change (8th cycle, 100-20-100% power changes, Case 2)

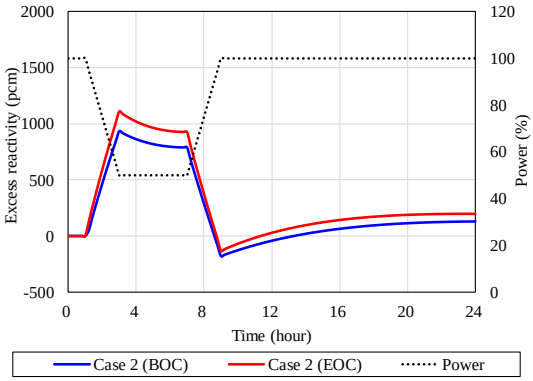

Fig. 13. The reactivity variation with power change (8th cycle, 100-50-100% power changes, Case 2)

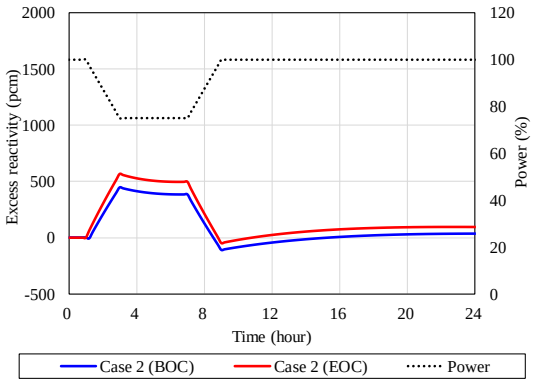

Fig. 14. The reactivity variation with power change (8th cycle, 100-75-100% power changes, Case 2)

3.2 Local Power Peaking Factor

By modulating the control rod positions to ensure a critical state at each power level, this analysis evaluated the variations in control rod insertion depths and the core peaking factors.

Fig. 15 through Fig. 19 illustrate the positions of the control rod banks R4 and R3 at each power level (100%, 80%, 60%, 40%, and 20%) in the 1st cycle and Table I and Table II summarized the Regulation Bank positions in the 1st cycle for the Case 1 and the Case 2.

Across the entire power range, except 100% power, the Case 1 maintained higher control rod positions compared to the Case 2, indicating a shallower insertion depth. This is because the RCS temperature program for the Case 1 stabilizes the average coolant temperature, thereby mitigating the massive positive reactivity insertion that occurs in Case 2 due to the sharp drop in the average coolant temperature and the strong negative MTC. At HFP, the control rod positions are identical because the coolant temperatures are the same.

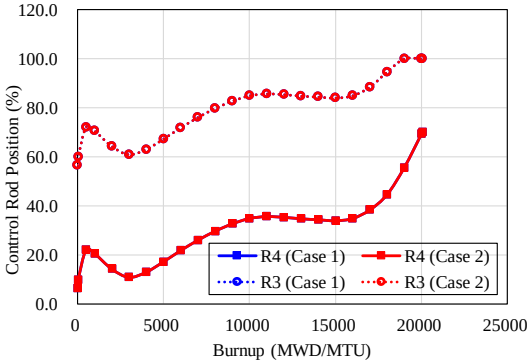

Fig. 15. Control rod positions versus burnup change at HFP (1st cycle)

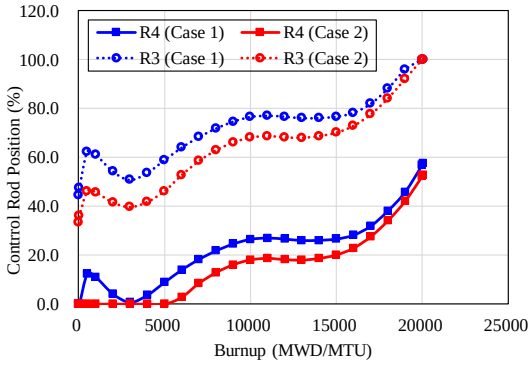

Fig. 16. Control rod positions versus burnup change at 80% power (1st cycle)

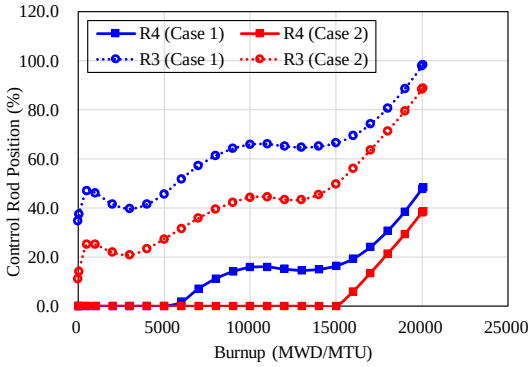

Fig. 17. Control rod positions versus burnup change at 60% power (1st cycle)

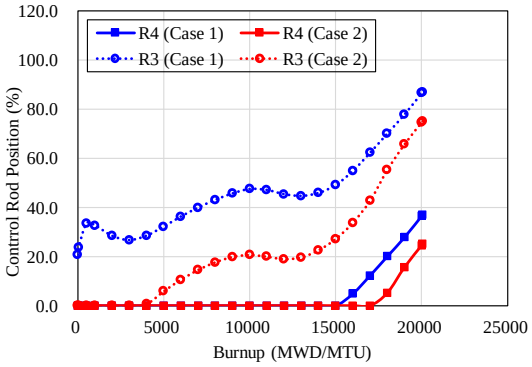

Fig. 18. Control rod positions versus burnup change at 40% power (1st cycle)

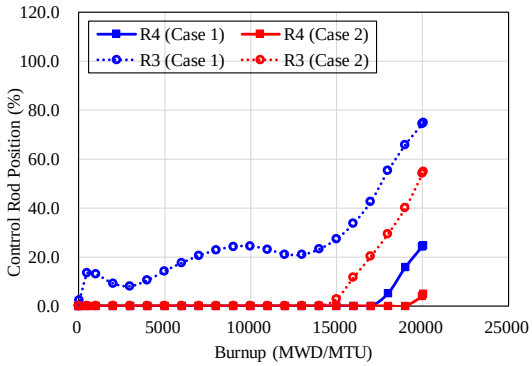

Fig. 19. Control rod positions versus burnup change at 20% power (1st cycle)

Consequently, as shown in Fig. 20 and Fig, 21, the Case 1 exhibited lower peakings compared to the Case 2 at the 1st cycle. The shallower rod insertion in the Case 1 effectively prevented the severe axial power distortion observed in the Case 2, where deep rod insertion induced a localized power concentration in the lower region of the core.

The discrepancy in peaking factors between the two cases becomes more pronounced as the core power level decreases. At 20% power, which is the lowest power level in this analysis, the Case 1 was evaluated at 2.354, whereas the Case 2 reached a higher value of 2.729.

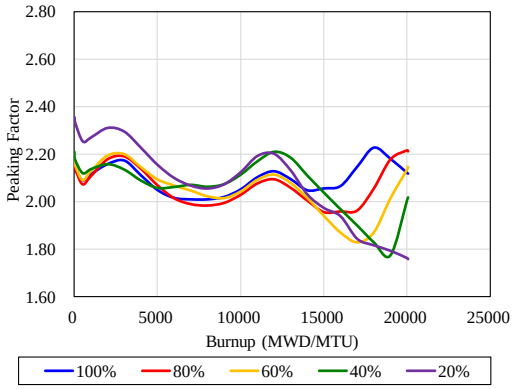

Fig. 20. Peaking factors versus burnup change (1st cycle, Case 1)

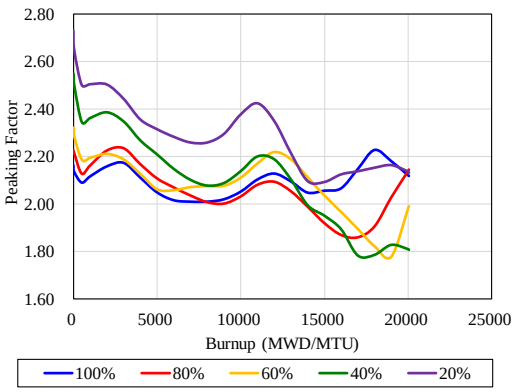

Fig. 21. Peaking factors versus burnup change (1st cycle, Case 2)

Fig. 22 through Fig. 26 depict the positions of the control rod banks R4 and R3 at each power level (100%, 80%, 60%, 40%, and 20%) in the 8th cycle and Table III and Table IV summarized the Regulation Bank positions in the 8th cycle for the Case 1and the Case 2. Consistent with the observations in the initial core cycle, the Case 1 maintained higher control rod positions compared to the Case 2.

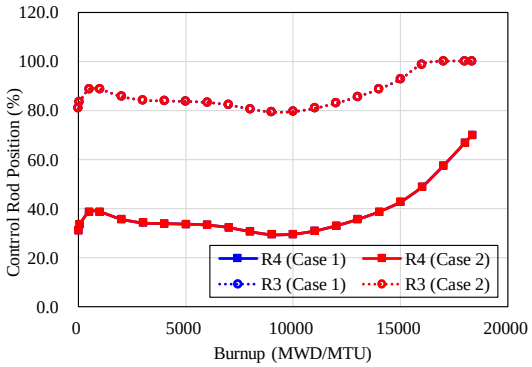

Fig. 22. Control rod positions versus burnup change at HFP (8th cycle)

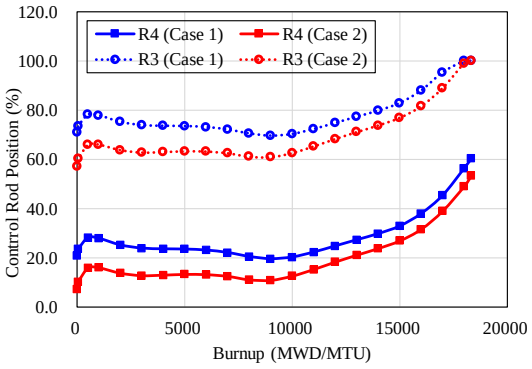

Fig. 23. Control rod positions versus burnup change at 80% power (8th cycle)

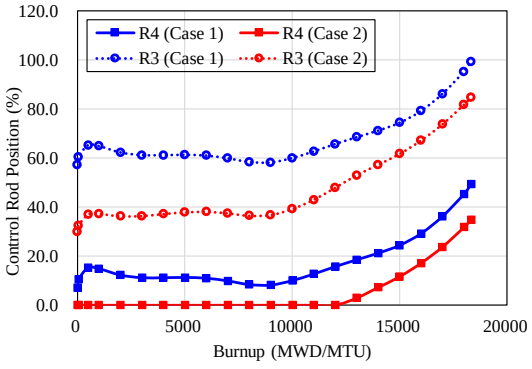

Fig. 24. Control rod positions versus burnup change at 60% power (8th cycle)

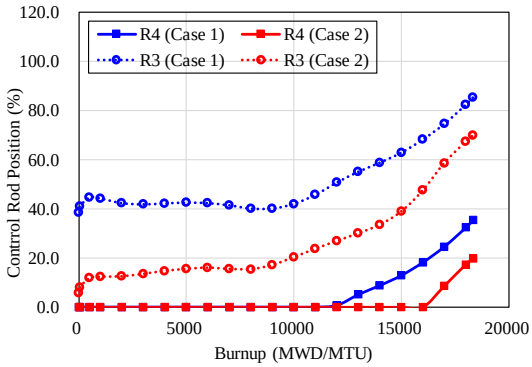

Fig. 25. Control rod positions versus burnup change at 40% power (8th cycle)

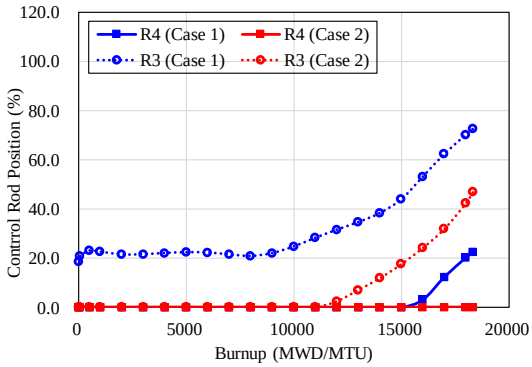

Fig. 26. Control rod positions versus burnup change at 20% power (8th cycle)

Consequently, as shown in Fig. 20 and Fig, 21, the Case 1 exhibited lower peaking factors compared to the Case 2 at the 8th cycle. The shallower rod insertion in the Case 1 effectively prevented the severe axial power distortion observed in the Case 2, where deep rod insertion induced a localized power concentration in the lower region of the core.

Consistent with the rod position data, Fig. 20 and Fig. 21 demonstrate that Case 1 yields lower peaking factors than Case 2. Lower core power levels lead to a more significant gap in peaking factor values between the cases. Specifically, at 20% power, the Case 1 exhibited a peaking factor of 2.351, while the Case 2 was calculated to be 2.534, reflecting the impact of deeper rod insertion.

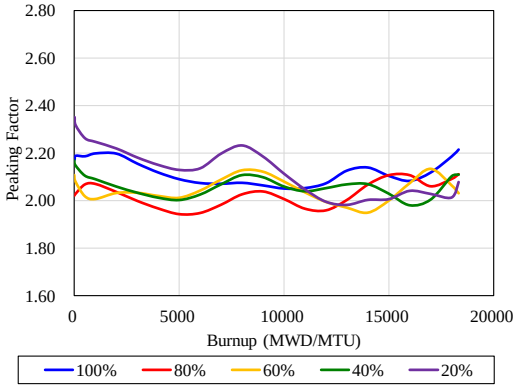

Fig. 27. Peaking factors versus burnup change (8th cycle, Case 1)

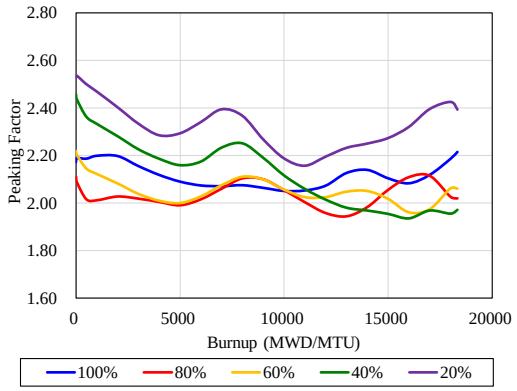

Fig. 28. Peaking factors versus burnup change (8th cycle, Case 2)

4. Conclusions

The numerical analysis of the daily load-follow operation confirms that the selection of an appropriate RCS temperature program is a critical factor for the stable operation of soluble boron-free SMR.

The results indicate a strong coupling between thermal-hydraulic feedback and neutronic stability. By adopting the sliding T_{in} strategy, the reactor can mitigate the reactivity swings driven by MTC effect, thereby allowing for shallower control rod insertion. This operational advantage directly translates into improved power peaking, particularly at low-power conditions where the discrepancy between sliding T_{in} concept and constant T_{in} concept peaked. These results demonstrate that the Sliding T_{in} strategy is superior in terms of maintaining core operational margins and power distribution stability.

Acknowledgement

This work was supported by the Innovative Small Modular Reactor Development Agency grant funded by the Korea Government (MCEE) (No. RS-2024-00405419).

REFERENCES

[1] Junggyu Lee et al., "The Feasibility of Controlling Secondary Reactivity Based on Coolant Temperature for Soluble Boron-free Operation", Transactions of Korea Nuclear Society Spring Meeting (2024).
[2] L. van der Merwe and C. J. Hah, "Reactivity balance for a soluble boron-free small modular reactor", Nuclear Engineering and Technology, Vol. 50, p. 723-731, Jul. 2018.
[3] K. S. Kim et al., "Transport Lattice Code KARMA 1.1," Transactions of Korea Nuclear Society Autumn Meeting (2009).
[4] K. S. Kim et al., "Implementation of the Gamma Transport Calculation Module in KARMA 1.2", Transactions of Korea Nuclear Society Spring Meeting (2011).
[5] T. Y. Han et al., "Verification of ASTRA Code with PWR MOX/UO2 Transient Benchmark Problem", Transactions of Korea Nuclear Society Autumn Meeting (2010).
[6] J. I. Yoon and H. G. Joo, "Two-Level Coarse Mesh Finite Difference Formulation with Multigroup Source Expansion Nodal Kernels", Journal of Nuclear Science and Technology, Vol. 45, p.668-682 (2008).
[7] H. G. Joo et al., "Multigroup pin power reconstruction with two-dimensional source expansion and corner flux discontinuity", Annals of Nuclear Energy, Vol. 36, p.85~97 (2009).

Table I. Control rod positions (1st cycle, Case 1)

Burnup	***R4***					***R3***					***R2***					***R1***				
	100	***80***	***60***	***40***	***20***	***100***	***80***	***60***	***40***	***20***	***100***	***80***	***60***	***40***	***20***	***100***	***80***	***60***	***40***	***20***
0	6.5	0.0	0.0	0.0	0.0	56.5	33.4	10.9	0.0	0.0	100.0	83.4	60.9	37.6	15.7	100.0	100.0	100.0	87.6	65.7
50	9.9	0.0	0.0	0.0	0.0	59.9	36.1	14.0	0.0	0.0	100.0	86.1	64.0	39.8	18.2	100.0	100.0	100.0	89.8	68.2
500	22.1	0.0	0.0	0.0	0.0	72.1	46.1	25.0	0.0	0.0	100.0	96.1	75.0	47.7	25.4	100.0	100.0	100.0	97.7	75.4
1000	20.6	0.0	0.0	0.0	0.0	70.6	45.7	25.0	0.0	0.0	100.0	95.7	75.0	48.5	25.9	100.0	100.0	100.0	98.5	75.9
2000	14.3	0.0	0.0	0.0	0.0	64.3	41.5	21.8	0.0	0.0	100.0	91.5	71.8	46.7	25.0	100.0	100.0	100.0	96.7	75.0
3000	10.9	0.0	0.0	0.0	0.0	60.9	39.7	20.7	0.0	0.0	100.0	89.7	70.7	47.1	25.8	100.0	100.0	100.0	97.1	75.8
4000	13.0	0.0	0.0	0.0	0.0	63.0	41.8	23.2	0.7	0.0	100.0	91.8	73.2	50.7	28.3	100.0	100.0	100.0	100.0	78.3
5000	17.2	0.0	0.0	0.0	0.0	67.2	46.2	27.2	5.9	0.0	100.0	96.2	77.2	55.9	31.3	100.0	100.0	100.0	100.0	81.3
6000	21.8	2.8	0.0	0.0	0.0	71.8	52.8	31.5	10.6	0.0	100.0	100.0	81.5	60.6	34.2	100.0	100.0	100.0	100.0	84.2
7000	26.0	8.5	0.0	0.0	0.0	76.0	58.5	35.7	14.6	0.0	100.0	100.0	85.7	64.6	36.7	100.0	100.0	100.0	100.0	86.7
8000	29.7	12.9	0.0	0.0	0.0	79.7	62.9	39.3	17.7	0.0	100.0	100.0	89.3	67.7	38.4	100.0	100.0	100.0	100.0	88.4
9000	32.7	16.1	0.0	0.0	0.0	82.7	66.1	42.1	19.9	0.0	100.0	100.0	92.1	69.9	39.3	100.0	100.0	100.0	100.0	89.3
10000	34.9	18.1	0.0	0.0	0.0	84.9	68.1	44.2	20.7	0.0	100.0	100.0	94.2	70.7	38.7	100.0	100.0	100.0	100.0	88.7
11000	35.7	18.7	0.0	0.0	0.0	85.7	68.7	44.4	20.0	0.0	100.0	100.0	94.4	70.0	37.2	100.0	100.0	100.0	100.0	87.2
12000	35.4	18.2	0.0	0.0	0.0	85.4	68.2	43.3	19.0	0.0	100.0	100.0	93.3	69.0	37.6	100.0	100.0	100.0	100.0	87.6
13000	34.8	18.0	0.0	0.0	0.0	84.8	68.0	43.3	19.7	0.0	100.0	100.0	93.3	69.7	40.6	100.0	100.0	100.0	100.0	90.6
14000	34.4	18.7	0.0	0.0	0.0	84.4	68.7	45.4	22.6	0.0	100.0	100.0	95.4	72.6	45.2	100.0	100.0	100.0	100.0	95.2
15000	34.0	20.1	0.0	0.0	0.0	84.0	70.1	49.6	27.2	2.8	100.0	100.0	99.6	77.2	52.8	100.0	100.0	100.0	100.0	100.0
16000	34.9	22.9	6.0	0.0	0.0	84.9	72.9	56.0	33.8	11.7	100.0	100.0	100.0	83.8	61.7	100.0	100.0	100.0	100.0	100.0
17000	38.4	27.6	13.5	0.0	0.0	88.4	77.6	63.5	42.8	20.3	100.0	100.0	100.0	92.8	70.3	100.0	100.0	100.0	100.0	100.0
18000	44.6	34.1	21.3	5.2	0.0	94.6	84.1	71.3	55.2	29.5	100.0	100.0	100.0	100.0	79.5	100.0	100.0	100.0	100.0	100.0
19000	55.6	42.1	29.3	15.7	0.0	100.0	92.1	79.3	65.7	40.1	100.0	100.0	100.0	100.0	90.1	100.0	100.0	100.0	100.0	100.0
20000	69.3	52.3	38.2	24.6	4.1	100.0	100.0	88.2	74.6	54.1	100.0	100.0	100.0	100.0	100.0	100.0	100.0	100.0	100.0	100.0
20055	70.0	52.9	38.7	25.1	4.9	100.0	100.0	88.7	75.1	54.9	100.0	100.0	100.0	100.0	100.0	100.0	100.0	100.0	100.0	100.0

Table II. Control rod positions (1st cycle, Case 2)

Burnup	***R4***					***R3***					***R2***					***R1***				
	100	***80***	***60***	***40***	***20***	***100***	***80***	***60***	***40***	***20***	***100***	***80***	***60***	***40***	***20***	***100***	***80***	***60***	***40***	***20***
0	6.5	0.0	0.0	0.0	0.0	56.5	44.6	34.6	20.7	0.0	100.0	94.6	84.6	70.7	48.6	100.0	100.0	100.0	100.0	98.6
50	9.9	0.0	0.0	0.0	0.0	59.9	47.5	37.4	23.7	2.3	100.0	97.5	87.4	73.7	52.3	100.0	100.0	100.0	100.0	100.0
500	22.1	12.3	0.0	0.0	0.0	72.1	62.3	46.8	33.4	13.4	100.0	100.0	96.8	83.4	63.4	100.0	100.0	100.0	100.0	100.0
1000	20.6	11.1	0.0	0.0	0.0	70.6	61.1	46.1	32.7	13.0	100.0	100.0	96.1	82.7	63.0	100.0	100.0	100.0	100.0	100.0
2000	14.3	4.2	0.0	0.0	0.0	64.3	54.2	41.5	28.4	9.1	100.0	100.0	91.5	78.4	59.1	100.0	100.0	100.0	100.0	100.0
3000	10.9	0.8	0.0	0.0	0.0	60.9	50.8	39.6	26.7	8.0	100.0	100.0	89.6	76.7	58.0	100.0	100.0	100.0	100.0	100.0
4000	13.0	3.7	0.0	0.0	0.0	63.0	53.7	41.4	28.5	10.5	100.0	100.0	91.4	78.5	60.5	100.0	100.0	100.0	100.0	100.0
5000	17.2	8.9	0.0	0.0	0.0	67.2	58.9	45.6	32.2	14.2	100.0	100.0	95.6	82.2	64.2	100.0	100.0	100.0	100.0	100.0
6000	21.8	14.0	1.7	0.0	0.0	71.8	64.0	51.7	36.3	17.6	100.0	100.0	100.0	86.3	67.6	100.0	100.0	100.0	100.0	100.0
7000	26.0	18.3	7.1	0.0	0.0	76.0	68.3	57.1	39.9	20.5	100.0	100.0	100.0	89.9	70.5	100.0	100.0	100.0	100.0	100.0
8000	29.7	21.8	11.2	0.0	0.0	79.7	71.8	61.2	43.1	22.8	100.0	100.0	100.0	93.1	72.8	100.0	100.0	100.0	100.0	100.0
9000	32.7	24.6	14.1	0.0	0.0	82.7	74.6	64.1	45.7	24.2	100.0	100.0	100.0	95.7	74.2	100.0	100.0	100.0	100.0	100.0
10000	34.9	26.5	15.8	0.0	0.0	84.9	76.5	65.8	47.5	24.4	100.0	100.0	100.0	97.5	74.4	100.0	100.0	100.0	100.0	100.0
11000	35.7	27.0	16.0	0.0	0.0	85.7	77.0	66.0	47.1	23.0	100.0	100.0	100.0	97.1	73.0	100.0	100.0	100.0	100.0	100.0
12000	35.4	26.6	15.1	0.0	0.0	85.4	76.6	65.1	45.4	21.1	100.0	100.0	100.0	95.4	71.1	100.0	100.0	100.0	100.0	100.0
13000	34.8	26.0	14.6	0.0	0.0	84.8	76.0	64.6	44.7	20.9	100.0	100.0	100.0	94.7	70.9	100.0	100.0	100.0	100.0	100.0
14000	34.4	26.1	15.0	0.0	0.0	84.4	76.1	65.0	45.9	23.2	100.0	100.0	100.0	95.9	73.2	100.0	100.0	100.0	100.0	100.0
15000	34.0	26.6	16.4	0.0	0.0	84.0	76.6	66.4	49.1	27.3	100.0	100.0	100.0	99.1	77.3	100.0	100.0	100.0	100.0	100.0
16000	34.9	28.2	19.3	4.9	0.0	84.9	78.2	69.3	54.9	33.7	100.0	100.0	100.0	100.0	83.7	100.0	100.0	100.0	100.0	100.0
17000	38.4	31.9	24.1	12.3	0.0	88.4	81.9	74.1	62.3	42.7	100.0	100.0	100.0	100.0	92.7	100.0	100.0	100.0	100.0	100.0
18000	44.6	38.1	30.6	20.1	5.2	94.6	88.1	80.6	70.1	55.2	100.0	100.0	100.0	100.0	100.0	100.0	100.0	100.0	100.0	100.0
19000	55.6	45.8	38.5	27.9	15.8	100.0	95.8	88.5	77.9	65.8	100.0	100.0	100.0	100.0	100.0	100.0	100.0	100.0	100.0	100.0
20000	69.3	56.9	47.8	36.6	24.4	100.0	100.0	97.8	86.6	74.4	100.0	100.0	100.0	100.0	100.0	100.0	100.0	100.0	100.0	100.0
20055	70.0	57.6	48.3	37.0	24.8	100.0	100.0	98.3	87.0	74.8	100.0	100.0	100.0	100.0	100.0	100.0	100.0	100.0	100.0	100.0

Table III. Control rod positions (8th cycle, Case 1)

Burnup	***R4***					***R3***					***R2***					***R1***				
	100	***80***	***60***	***40***	***20***	***100***	***80***	***60***	***40***	***20***	***100***	***80***	***60***	***40***	***20***	***100***	***80***	***60***	***40***	***20***
0	31.0	7.2	0.0	0.0	0.0	81.0	57.2	29.9	5.7	0.0	100.0	100.0	79.9	55.7	30.7	100.0	100.0	100.0	100.0	80.7
50	33.5	10.3	0.0	0.0	0.0	83.5	60.3	32.4	8.1	0.0	100.0	100.0	82.4	58.1	32.6	100.0	100.0	100.0	100.0	82.6
500	38.7	15.9	0.0	0.0	0.0	88.7	65.9	36.9	11.8	0.0	100.0	100.0	86.9	61.8	34.6	100.0	100.0	100.0	100.0	84.6
1000	38.6	16.0	0.0	0.0	0.0	88.6	66.0	37.2	12.3	0.0	100.0	100.0	87.2	62.3	34.8	100.0	100.0	100.0	100.0	84.8
2000	35.7	13.8	0.0	0.0	0.0	85.7	63.8	36.2	12.5	0.0	100.0	100.0	86.2	62.5	35.2	100.0	100.0	100.0	100.0	85.2
3000	34.2	12.8	0.0	0.0	0.0	84.2	62.8	36.3	13.5	0.0	100.0	100.0	86.3	63.5	36.3	100.0	100.0	100.0	100.0	86.3
4000	33.9	13.0	0.0	0.0	0.0	83.9	63.0	37.1	14.7	0.0	100.0	100.0	87.1	64.7	37.5	100.0	100.0	100.0	100.0	87.5
5000	33.7	13.3	0.0	0.0	0.0	83.7	63.3	37.8	15.5	0.0	100.0	100.0	87.8	65.5	38.3	100.0	100.0	100.0	100.0	88.3
6000	33.3	13.2	0.0	0.0	0.0	83.3	63.2	38.0	16.0	0.0	100.0	100.0	88.0	66.0	38.3	100.0	100.0	100.0	100.0	88.3
7000	32.3	12.5	0.0	0.0	0.0	82.3	62.5	37.4	15.5	0.0	100.0	100.0	87.4	65.5	37.8	100.0	100.0	100.0	100.0	87.8
8000	30.6	11.1	0.0	0.0	0.0	80.6	61.1	36.4	15.4	0.0	100.0	100.0	86.4	65.4	38.3	100.0	100.0	100.0	100.0	88.3
9000	29.4	10.9	0.0	0.0	0.0	79.4	60.9	36.7	17.1	0.0	100.0	100.0	86.7	67.1	40.5	100.0	100.0	100.0	100.0	90.5
10000	29.6	12.6	0.0	0.0	0.0	79.6	62.6	39.1	20.3	0.0	100.0	100.0	89.1	70.3	43.7	100.0	100.0	100.0	100.0	93.7
11000	30.9	15.3	0.0	0.0	0.0	80.9	65.3	42.9	23.7	0.0	100.0	100.0	92.9	73.7	47.6	100.0	100.0	100.0	100.0	97.6
12000	33.0	18.3	0.0	0.0	0.0	83.0	68.3	47.8	26.9	2.4	100.0	100.0	97.8	76.9	52.4	100.0	100.0	100.0	100.0	100.0
13000	35.6	21.1	2.9	0.0	0.0	85.6	71.1	52.9	30.0	7.0	100.0	100.0	100.0	80.0	57.0	100.0	100.0	100.0	100.0	100.0
14000	38.7	23.8	7.2	0.0	0.0	88.7	73.8	57.2	33.5	11.8	100.0	100.0	100.0	83.5	61.8	100.0	100.0	100.0	100.0	100.0
15000	42.7	26.9	11.6	0.0	0.0	92.7	76.9	61.6	38.9	17.5	100.0	100.0	100.0	88.9	67.5	100.0	100.0	100.0	100.0	100.0
16000	48.8	31.6	17.1	0.0	0.0	98.8	81.6	67.1	47.5	24.1	100.0	100.0	100.0	97.5	74.1	100.0	100.0	100.0	100.0	100.0
17000	57.4	39.0	23.7	8.6	0.0	100.0	89.0	73.7	58.6	31.8	100.0	100.0	100.0	100.0	81.8	100.0	100.0	100.0	100.0	100.0
18000	66.7	49.0	31.7	17.3	0.0	100.0	99.0	81.7	67.3	42.3	100.0	100.0	100.0	100.0	92.3	100.0	100.0	100.0	100.0	100.0
18335	70.0	53.3	34.7	19.8	0.0	100.0	100.0	84.7	69.8	46.9	100.0	100.0	100.0	100.0	96.9	100.0	100.0	100.0	100.0	100.0

Table IV. Control rod positions (8th cycle, Case 2)

Burnup	***R4***					***R3***					***R2***					***R1***				
	100	***80***	***60***	***40***	***20***	***100***	***80***	***60***	***40***	***20***	***100***	***80***	***60***	***40***	***20***	***100***	***80***	***60***	***40***	***20***
0	31.0	20.9	7.1	0.0	0.0	81.0	70.9	57.1	38.5	18.4	100.0	100.0	100.0	88.5	68.4	100.0	100.0	100.0	100.0	100.0
50	33.5	23.5	10.4	0.0	0.0	83.5	73.5	60.4	41.1	20.8	100.0	100.0	100.0	91.1	70.8	100.0	100.0	100.0	100.0	100.0
500	38.7	28.2	15.2	0.0	0.0	88.7	78.2	65.2	44.6	23.0	100.0	100.0	100.0	94.6	73.0	100.0	100.0	100.0	100.0	100.0
1000	38.6	27.9	14.8	0.0	0.0	88.6	77.9	64.8	44.2	22.5	100.0	100.0	100.0	94.2	72.5	100.0	100.0	100.0	100.0	100.0
2000	35.7	25.2	12.2	0.0	0.0	85.7	75.2	62.2	42.3	21.4	100.0	100.0	100.0	92.3	71.4	100.0	100.0	100.0	100.0	100.0
3000	34.2	23.9	11.1	0.0	0.0	84.2	73.9	61.1	41.8	21.5	100.0	100.0	100.0	91.8	71.5	100.0	100.0	100.0	100.0	100.0
4000	33.9	23.6	11.1	0.0	0.0	83.9	73.6	61.1	42.2	22.0	100.0	100.0	100.0	92.2	72.0	100.0	100.0	100.0	100.0	100.0
5000	33.7	23.5	11.2	0.0	0.0	83.7	73.5	61.2	42.5	22.3	100.0	100.0	100.0	92.5	72.3	100.0	100.0	100.0	100.0	100.0
6000	33.3	23.1	10.9	0.0	0.0	83.3	73.1	60.9	42.3	22.2	100.0	100.0	100.0	92.3	72.2	100.0	100.0	100.0	100.0	100.0
7000	32.3	22.1	9.8	0.0	0.0	82.3	72.1	59.8	41.4	21.4	100.0	100.0	100.0	91.4	71.4	100.0	100.0	100.0	100.0	100.0
8000	30.6	20.5	8.3	0.0	0.0	80.6	70.5	58.3	40.1	20.8	100.0	100.0	100.0	90.1	70.8	100.0	100.0	100.0	100.0	100.0
9000	29.4	19.6	8.1	0.0	0.0	79.4	69.6	58.1	40.1	22.0	100.0	100.0	100.0	90.1	72.0	100.0	100.0	100.0	100.0	100.0
10000	29.6	20.3	9.9	0.0	0.0	79.6	70.3	59.9	42.0	24.7	100.0	100.0	100.0	92.0	74.7	100.0	100.0	100.0	100.0	100.0
11000	30.9	22.3	12.6	0.0	0.0	80.9	72.3	62.6	45.7	28.2	100.0	100.0	100.0	95.7	78.2	100.0	100.0	100.0	100.0	100.0
12000	33.0	24.8	15.6	0.7	0.0	83.0	74.8	65.6	50.7	31.5	100.0	100.0	100.0	100.0	81.5	100.0	100.0	100.0	100.0	100.0
13000	35.6	27.3	18.4	5.1	0.0	85.6	77.3	68.4	55.1	34.6	100.0	100.0	100.0	100.0	84.6	100.0	100.0	100.0	100.0	100.0
14000	38.7	29.8	21.1	8.8	0.0	88.7	79.8	71.1	58.8	38.3	100.0	100.0	100.0	100.0	88.3	100.0	100.0	100.0	100.0	100.0
15000	42.7	32.9	24.3	12.9	0.0	92.7	82.9	74.3	62.9	43.9	100.0	100.0	100.0	100.0	93.9	100.0	100.0	100.0	100.0	100.0
16000	48.8	38.0	29.1	18.2	3.1	98.8	88.0	79.1	68.2	53.1	100.0	100.0	100.0	100.0	100.0	100.0	100.0	100.0	100.0	100.0
17000	57.4	45.4	36.1	24.6	12.3	100.0	95.4	86.1	74.6	62.3	100.0	100.0	100.0	100.0	100.0	100.0	100.0	100.0	100.0	100.0
18000	66.7	56.4	45.2	32.4	20.1	100.0	100.0	95.2	82.4	70.1	100.0	100.0	100.0	100.0	100.0	100.0	100.0	100.0	100.0	100.0
18335	70.0	60.3	49.2	35.4	22.5	100.0	100.0	99.2	85.4	72.5	100.0	100.0	100.0	100.0	100.0	100.0	100.0	100.0	100.0	100.0